Casarotto, Silvia; Fecchio, Matteo; Rosanova, Mario; Varone, Giuseppe; D'Ambrosio, Sasha; Sarasso, Simone; Pigorini, Andrea; Russo, Simone; Comanducci, Angela; Ilmoniemi, Risto J.; Massimini, Marcello

The rt-TEP tool: real-time visualization of TMS-Evoked Potentials to maximize cortical activation and minimize artifacts

The rt-TEP tool: real-time visualization of TMS-Evoked Potentials to maximize cortical activation and minimize artifacts

Silvia Casarotto [a,b,*], Matteo Fecchio [a,c], Mario Rosanova [a], Giuseppe Varone [d], Sasha D'Ambrosio [a], Simone Sarasso [a], Andrea Pigorini [a], Simone Russo [a], Angela Comanducci [b], Risto J. Ilmoniemi [e], Marcello Massimini [a,b,*]

[a] *Department of Biomedical and Clinical Sciences "L. Sacco", University of Milan, Milan, Italy*
[b] *Fondazione Don Carlo Gnocchi ONLUS, Milan, Italy*
[c] *Center for Neurotechnology and Neurorecovery, Department of Neurology, Massachusetts General Hospital, Boston, MA, USA*
[d] *Department of Neuroscience, Imaging and Clinical Science, "G. D'Annunzio" University of Chieti-Pescara, Chieti, Italy*
[e] *Department of Neuroscience and Biomedical Engineering, Aalto University School of Science, Espoo, Finland*

1. Introduction

Transcranial magnetic stimulation (TMS) can directly activate the cerebral cortex with a huge number of parameter combinations such as position, orientation, and intensity of the induced electric field (E-field). This flexibility offers unprecedented opportunities for exploring and modulating cortical excitability but also represents a challenge; when a TMS coil is positioned on the scalp region overlying a cortical area of interest, the actual impact of the E-field on cortical neurons is very hard to predict. Indeed, even when individual head models provided by state-of-the-art TMS navigation systems are available as a priori information, key factors such as microscale axon orientation, cytoarchitectonics and local neuronal excitability remain unaccounted for and may dramatically affect the interaction between the induced E-field and brain activity.

For this reason, when targeting the primary motor cortex (M1), TMS stimulation parameters (coil position, coil orientation, intensity) are initially set based on coarse a priori anatomical information (Silva et al., 2021) and then adjusted post-hoc, until the electromyographic (EMG) activity recorded from a selected target muscle satisfies standard latency

and amplitude requirements (Rossini et al., 2015). Hence, despite the potential confound represented by changes in the excitability of spinal motor neurons, motor-evoked potentials have so far represented the standard real-time feedback for titrating TMS parameters in research, diagnostic and treatment protocols.

However, when stimulating outside the primary motor cortex such immediate readout is not available, thus preventing a reliable control over whether, or how effectively, TMS is impacting cortical neurons. This lack of control represents a fundamental limitation not only for TMS protocols aimed at inducing plasticity but also for studies in which TMS is employed in combination with other techniques to assess the state of cortical circuits. For example, differences in the strength of direct cortical activation have been highlighted as a major problem affecting the reproducibility of studies employing TMS in combination with electroencephalography (TMS-EEG) to probe cortical excitability and connectivity (Belardinelli et al., 2019). Clearly, maximizing the direct impact of stimulation on cortical neurons while minimizing collateral effects such as cranio-facial muscle, magnetic or sensory activations is a key prerequisite for improving the reproducibility across laboratories, the signal-to-noise ratio (SNR) and the informativeness of

TMS–EEG studies. Towards this aim, in our previous TMS–EEG works, we have used visualization software to set stimulation parameters in real time based on the quality and amplitude of the EEG response to TMS (Casali et al., 2010; Casarotto et al., 2016; Rosanova, Fecchio et al., 2018; Sinitsyn et al., 2020). Such software tools were either implemented on EEG systems that are now out of production (eXimia EEG, Nexstim Plc, Finland) or based on hardware/software solutions that were customized to our specific set-up and are thus not available to the larger community.

Here, we present rt-TEP (real-time TMS-Evoked Potential), an open-source, Matlab®-based software tool that allows quantifying in real time the direct impact of TMS on potentially any cortical area while minimizing common confounds, such as auditory-related activations. Using rt-TEP, the operator can (*i*) effectively inspect single-trial data to detect and minimize early artifacts (magnetic and cranio-facial muscle twitches) by small adjustments of coil position and orientation, (*ii*) visualize in real time the amplitude of the early (8–50 ms) TEP after averaging in real time a limited number (e.g., 10–30) of trials, (*iii*) use this feedback to titrate TMS to achieve a desired level of initial cortical activation and (*iv*) estimate the overall response quality. By offering a clear visualization of the early (8–50 ms) EEG response in informative, interactive displays, rt-TEP guides the operator in setting stimulation parameters to ensure a controlled level of cortical activation during the experiment. Further, by providing an immediate view of the overall response at later latencies, rt-TEP can be used to adjust other relevant experimental settings (e.g., loudness and/or spectral features of the noise masking; see Russo et al., 2022) in order to minimize the contribution of auditory-evoked potentials. rt-TEP interfaces with the most widely used TMS-compatible EEG amplifiers. Source code is released (*https://github.com/iTCf/rt-TEP.git*) under GNU General Public License

v3.0, which allows the user to extend the compatibility of this software to other EEG amplifiers.

2. Real-time control of TEPs with rt-TEP: rationale and procedures

rt-TEP software must be installed on a client computer (Windows, Mac or Linux OS) that receives real-time data streaming via ethernet from a server computer, which is in turn directly connected to the EEG amplifier and runs a proprietary software responsible for data collection and storage. As a first step, rt-TEP guides the operator through a series of interactive windows to select the EEG amplifier in use (Figure S1A). Currently, four different amplifiers can be selected: BrainAmp (Brain Products GmbH, Germany), g.HIamp (G.TEC Medical Engineering GmbH, Austria), eego™ mylab (ANT Neuro, Netherlands) and Bittium NeurOne™ Tesla (Bittium Corporation, Finland).

Then, rt-TEP requires one to specify the settings for connecting with the server computer (e.g., IP address) and for the desired data display (e. g., layout of the recording channels, temporal windows of interest, sampling rate) (Figure S1B). In principle, any arbitrary set of EEG and EOG (electrooculographic) recording channels can be specified and visualized (Figure S1C); additional channels connected to the same amplifier, such as electrocardiographic channels, must be included in the recording channels layout although are not displayed by rt-TEP.

Once connected to the amplifier, rt-TEP automatically displays continuous raw EEG data (see arrow 1 in Fig. 1) to check for successful real-time data streaming. At this point, rt-TEP is ready to display TEP features. This can be done by activating two different interactive visualization modes (see arrow 2 and arrow 3 in Fig. 1; see Supplementary methods for detailed description of data recording procedure), updated
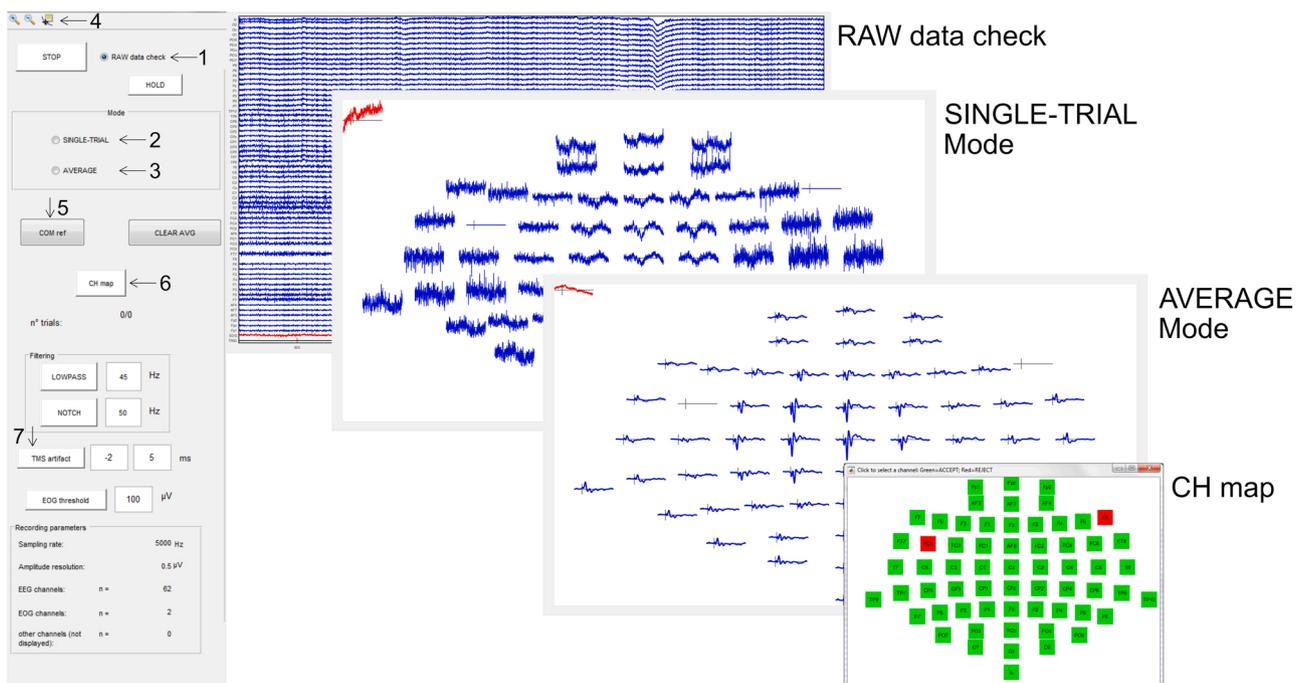
Fig. 1. The main control panel of rt-TEP (left) and the three different displays that can be alternatively activated, including RAW data check, SINGLE-TRIAL Mode and AVERAGE Mode. In the topographic arrangement view, data are displayed in average reference by default; however, common physical reference can be retrieved by pressing the button COM ref. Zooming and measuring tools can be activated through the buttons on the top left menu bar (arrow 4). Button *CH map* opens an interface (shown in the bottom right corner) that allows to individually reject single-channel data from the display as well as from the computation of the average reference. When the TMS artifact button is activated, a selectable time window around TMS pulses is replaced with a constant value to mask the pulse artifact. In addition, rt-TEP can apply LOWPASS and NOTCH filtering in real time to both single-trial and average data; when the EOG threshold button is activated, single trials with an EOG amplitude exceeding a selectable value are automatically excluded from the averaging process.

in real time after each TMS pulse. Used sequentially, these modes guide the operator through a series of steps to optimize stimulation parameters before starting the actual measurement. As described in more details below, the first mode allows an informative inspection of single-trial responses that is instrumental to (*i*) mask the pulse artifact, (*ii*) compute the average reference after the rejection of bad channels, (*iii*) assess the potential presence of the recharge artifact and remove it from the window of interest, (*iv*) detect, locate and correct potential discharge artifacts, and (*v*) detect, locate and avoid/minimize potential artifacts from cranio-facial muscle activation. Once all the artifacts affecting the early post-stimulus time interval have been identified and minimized by the user, the second mode, which displays average data, offers a quantitative evaluation of the impact of TMS on cortical neurons. This is the critical step in which the operator can further refine the stimulation parameters to ensure that the early EEG response to TMS is present and falls within the desired amplitude range, and that no obvious sensory-related artifacts are present. In typical conditions, this EEG-guided parameter search lasts for about 10 min from the initial coil positioning on the area of interest. In what follows, we illustrate this process and explain its rationale by using practical examples and real data.

2.1. SINGLE-TRIAL mode: minimization of short-latency artifacts

In single-trial mode, rt-TEP shows EEG epochs of specified duration around the TMS pulse (e.g., from −100 to +400 ms), refreshing at every stimulus: EEG channels are displayed in a topographic arrangement and signals can be easily explored through simple zooming and measuring tools (see arrow 4 in Fig. 1). This mode enables the user to quickly detect and avoid artifacts that contaminate the initial portion of the post-stimulus EEG, as illustrated in detail below.

2.1.1. Pulse artifact

During TMS pulse delivery, the transient (a few hundreds of μs) flow of current in the coil, peaking at several kA (Koponen et al., 2015), induces a large voltage in the EEG leads, which is proportional to the time rate of the magnetic flux threading the loop formed by the positive and negative input of the EEG amplifier, along the wires to the electrodes and via the head. Typically, a customized electrode shape is employed to prevent the induction of eddy currents in the electrodes themselves (e.g., pellet-wise, wire-wise, ring-wise with a slit) (Virtanen et al., 1999). The pulse artifact's duration can be further reduced (down to a few milliseconds) by setting optimal acquisition parameters of the EEG amplifier, such as wide measuring range (tens of mV), a large hardware filtering bandwidth (up to several kHz) and a high sampling rate (several kHz). Even when these procedures are in place, the electromagnetic artifact is still several orders of magnitude larger than brain activity and hampers the real-time assessment of the early EEG response to TMS (Figure S2).

As a first step, rt-TEP allows one to remove the large pulse artifact from the online visualization by replacing the real signal with a constant value within a selectable time window around pulse delivery (see arrow 7 in Fig. 1). As an example, using the BrainAmp DC amplifier (Brain Products GmbH, Germany) with 16.384 mV measuring range (16 bit A/D converter, 0.5 μV resolution per bit), DC-to-1-kHz hardware filtering bandwidth and 5-kHz sampling rate, the pulse artifact can be effectively removed by setting the time window to be replaced with a constant value from –2 to + 5 ms with respect to the pulse (Fig. 2A, B). Once the large pulse artifact is eliminated, the *y*-axis range can be uniformly rescaled to proceed with a more fine-scaled inspection of the EEG signal.

2.1.2. From common physical reference to average reference: rejecting bad channels

The data streamed out by the amplifiers are obtained as potential differences between each measuring electrode and a unique "reference"

Examples of non-physiological artifacts on single-trial data
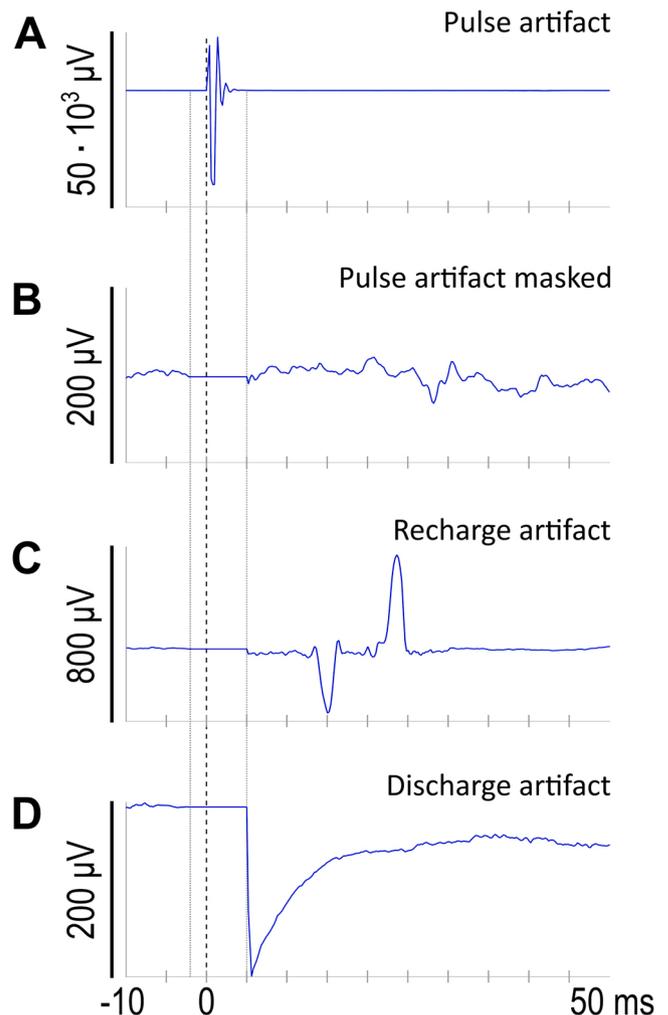
Fig. 2. Examples of non-physiological artifacts visible on single-channel, single-trial data: pulse artifact in common physical reference before (A) and after (B) masking, recharge artifact in average reference (C) and discharge artifact in average reference (D). For the all-channels display, see Figures S2, S3 and S4.

electrode. These unipolar EEG recordings are inevitably affected by the location of the physical reference due to the lack of a "neutral" reference site anywhere in the body (Lei and Liao, 2017; Nunez and Srinivasan, 2006). Hence, the time course of either single-trial or average data in common reference results in an artificially high degree of correlation across channels. This prevents the detection of artifacts with a characteristic spatial distribution, the discrimination between widespread artifacts and common mode signals, and ultimately the evaluation of the topography of genuine EEG responses to TMS. In principle, the average reference, which consists in subtracting from each EEG recording a linear combination of the recordings from all electrodes, successfully mitigates the bias of unipolar reference, provides better spatial information and a more reliable estimation of the signal amplitude (Nunez, 2010; Yao et al., 2019). However, a reliable average reference montage requires that bad channels that are either saturated, disconnected, or contaminated by irreducible artifacts, are not considered; otherwise, artifacts would naturally spread across all the recording electrodes and/or the signal would be artificially injected into channels that are not

picking up any electrical activity either because they are disconnected or saturated. In order to compute a reliable average reference, rt-TEP implements a simple interface to reject bad channels in real time (see arrow 6 in Fig. 1): rejected channels are excluded from the computation of the average reference and are not displayed. The detection of bad channels can be performed both in average reference and in common reference, since rt-TEP allows switching between these two montages with just a button press (see arrow 5 in Fig. 1). This is important because in case abnormal activity in some channels has such a large amplitude to contaminate all the other channels when computing the average reference, the detection of bad channels can be better performed by switching to common reference. For example, this kind of montage allows detecting outlier channels that are either heavily contaminated by artifacts (e.g., because of a loose contact) or flat (e.g., due to amplifier saturation). Such flexibility in the exploration and rejection of bad channels is not available in typical commercial acquisition software and is a prerequisite for the following steps as it allows visualizing average-reference EEG potentials in real time with unprecedented clarity.

2.1.3. Recharge artifact

After zero-padding the pulse artifact and re-referencing, the third step involves inspecting the signal for other sources of artifact such as the recharge artifact. Indeed, EEG amplifiers may be also disturbed by the recharging of the stimulator's capacitors between subsequent pulses; this occurs when there is a transient current flow or a change in the potential of the coil during the recharging. The occurrence of this artifact can be readily identified on the single-trial display provided by rt-TEP, once the pulse artifact is eliminated (Figure S3). The waveform of this artifact may change with the characteristics of the TMS unit, the coil type, and the stimulation intensity. Fig. 2C shows an example of the recharge artifact produced by the Rapid[2] stimulator (Magstim Ltd, UK) equipped with a D70 Remote Coil. By default, the stimulator's capacitors are usually recharged immediately after pulse delivery, thus possibly contaminating early EEG responses to TMS. If not detected before acquisition, the presence of a recharge artifact within a time-window of interest can irreversibly corrupt the measurement.

If present, the recharge artifact can be removed from the window of interest by delaying via software on the TMS unit the time of recharging. As an example, when stimulating at an inter-pulse interval randomly jittered between 2 and 2.3 s, the operator could set the time of recharging between 900 and 1000 ms after the pulse in order to get the largest symmetric artifact-free temporal window around TMS. Most TMS units offer the possibility to adjust the timing of the recharge artifact, which represents a useful experimental workaround to prevent the contamination of TEPs and thus the resorting to analytical procedures for recovering the signal of interest.

2.1.4. Discharge artifact

Electromagnetic pulses may also charge stray or material-boundary capacitances located along any possible induction current path, e.g., at the electrode–gel and gel–skin interfaces. In particular, the area covered by the conductive gel and the aqueous ionic extracellular space of deep skin layers, separated by the stratum corneum of the epidermis acting as a hydrophobic dielectric, forms a capacitor (Freche et al., 2018). Immediately after being charged by the pulse, these capacitances discharge and produce a non-exponentially decaying artifact on the recorded signal, which can last several tens of ms. Figure S4 shows how this artifact appears on the single-trial display provided by rt-TEP after masking the pulse artifact (Fig. 2D displays a representative channel).

The discharge artifact can be prevented by carefully lowering the resistance of the outermost layer of the epidermis and by using EEG electrodes with a shape that has been specifically designed to facilitate

skin preparation. In particular, it is important (*i*) to move the hair from the scalp surface in direct contact with the electrode, (*ii*) to scrub the skin with an abrasive paste and (*iii*) to finally inject as much gel as necessary between the skin and the electrode. In case a decay artifact is still present, a further refinement of electrode impedance may be helpful in reducing its amplitude.

2.1.5. Muscle artifact

The interaction between TMS pulses and excitable head tissues, such as muscular fibers and peripheral nerves, may produce additional artifacts that are superimposed on the brain responses due to direct perturbation of cortical neurons. Indeed, TMS pulses may induce craniofacial muscles to twitch by either the depolarization of intramuscular nerve endings close to the neuromuscular junction or by the activation of their nerves. The resulting electromyographic signals, recorded by the EEG electrodes, can be several orders of magnitude larger than neuronal signals and can last tens of ms. Once the pulse, recharge and discharge artifacts are eliminated, rt-TEP enables a straightforward detection of muscle artifacts. Their waveform is usually characterized by a biphasic deflection, peaking at 5–10 ms and at 8–20 ms post-stimulus, followed by a slow return to the baseline level at around 40–50 ms (Mutanen et al., 2013; Mäki and Ilmoniemi, 2011). Since cranio-facial muscles are mostly located over the frontolateral and occipital aspects of the head, EEG responses to TMS are less susceptible to muscle artifacts when pulses are delivered over dorsal regions close to the midline (Mutanen et al., 2013).

When targeting sites located away from the medial aspect of the head, the likelihood of supra-threshold activation of cranio-facial muscles by TMS depends on the stimulation intensity and on the angle between the main direction of muscle fibers and of the induced E-field. Fig. 3 shows two representative single-trial EEG responses to TMS (zoom on frontocentral channels; for the all-channels display see Figure S5) obtained by stimulating the same cortical site, at the same intensity, but with a different orientation of the coil: the muscle artifact clearly visible in Fig. 3A is greatly reduced by simply rotating the coil 30° clockwise (Fig. 3B). Although a complete obliteration of this kind of artifact may not be possible in all recordings, an EEG-informed fine-tuning of TMS parameters can be greatly effective without compromising the level of cortical activation. Minimizing muscle twitches before starting the measurements is very important for at least two reasons. First, it prevents the superimposition of electromyographic activity on the EEG signal, thus allowing to visualize the early components (within the first 50 ms) of the EEG response to TMS, which are key for titrating the final stimulation parameters (see paragraph 2.2). Second, because they are clearly perceived by the examined subject, thus potentially resulting in unspecific brain responses to sensory stimulation (Conde et al., 2019) or to the activation of the saliency network (Rocchi et al., 2021).

In conclusion, different artifacts can mask the initial brain responses to direct cortical stimulation with TMS. The single-trial display mode provided by rt-TEP guides the operator through a series of steps in which these artifacts can be recognized and eliminated. Once this is done, the TMS operator can move to the average display mode to visualize, quantify, and optimize the effects of TMS on the underlying circuits, before performing the actual measurement.

2.2. AVERAGE MODE: maximizing the signal-to-noise ratio of TEPs

In the average mode, rt-TEP provides real-time feedback about the amplitude, morphology and topography of the average EEG response evoked by TMS. In this setting, the operator can visualize in real time with unprecedented clarity the build-up of TEPs and can evaluate the quality of evoked components already after averaging a few tens of trials. Specifically, the user can (*i*) ascertain whether the TEPs are
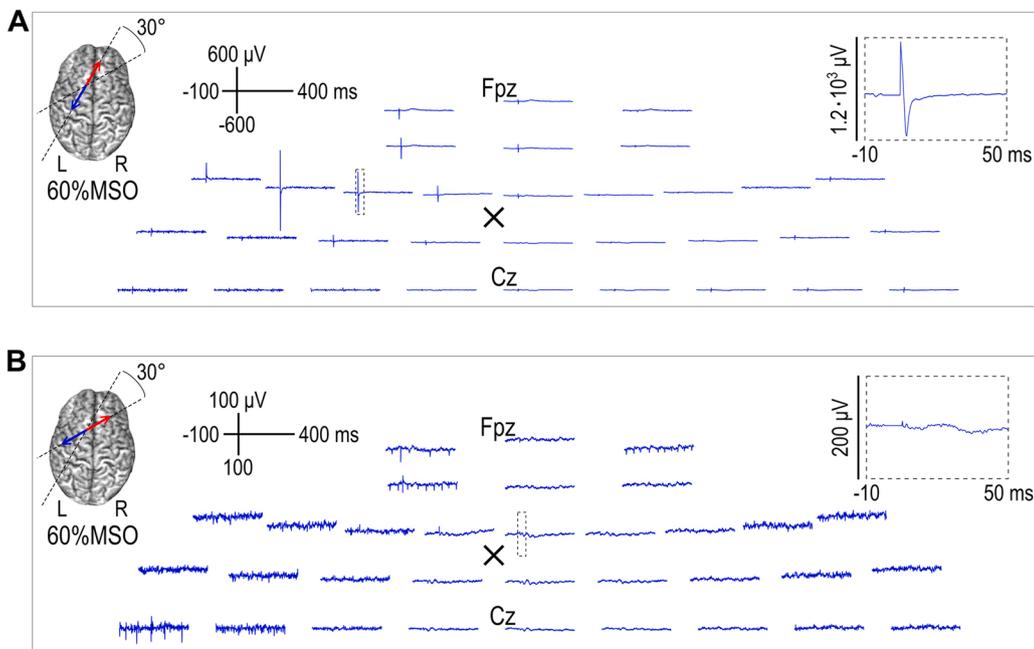
Fig. 3. Single-trial EEG responses to TMS applied on the left frontal cortex (black cross) at 60%MSO (zoom on frontocentral channels): the orientation of the induced E-field differs by 30° between panels A and B, as depicted on a rendered brain. The pulse artifact has been visually masked by replacing the signal between − 2 and + 5 ms with a constant value. EEG data were collected with a BrainAmp DC amplifier and TMS was delivered with an NBS4 Nexstim system. MSO = maximum stimulator output; L = left; R = right.

characterized by features that are consistent with an EEG response to direct cortical stimulation and (*ii*) quantify the strength and location of the initial (8–50 ms) neuronal response. If the visualized TEPs meet the desired criteria (see the next Section 2.2.1), the operator can start the measurements and data collection with a full set of trials (typically at least 100). Otherwise, she/he can further refine stimulation parameters. Below, we illustrate, using data obtained during a typical experiment, how rt-TEP can guide the operator in this decision process towards the maximization of the SNR of TEPs.

2.2.1. Using rt-TEP during a typical experiment

We here describe a typical experiment in which rt-TEP is used as a visual guide to titrate TMS parameters to a desired endpoint set by the user. The specific endpoint (i.e., the desired amplitude of the early and local TEPs) may vary depending on the goal of the experimenter and can be set based on different criteria. While in the Supplementary results we present a more sophisticated method that takes into account the variability of spontaneous EEG to achieve a desired SNR, in the following we describe a simpler case where the target amplitude is set at a fixed level to illustrate the general workflow and capability of rt-TEP.

In this example, the user specifically wants to achieve the same target amplitude obtained in previous studies when stimulating the premotor cortex of healthy controls (Fig. 4 in Rosanova et al., 2009, black traces). These responses are characterized by high-amplitude (peak-to-peak amplitude $V_{pp} > 10$ μV) early (8–50 ms) components in the EEG channels located underneath the TMS coil. In addition, they show a visible topographical asymmetry, with larger early components in the channels ipsilateral to the stimulation site as compared to homologous contralateral channels. These TEP features are different from those reported by other studies in healthy subjects (see for example the comparison in Fig. 1 in Belardinelli et al., 2019) and are also a key requirement for studies in brain-injured patients (Casarotto et al., 2016; Rosanova et al., 2018; Sarasso et al., 2020), in which similar amplitude criteria (early and local components $V_{pp} > 10$ μV) are set to warrant high SNR for subsequent computation of complexity indices (PCI - Perturbational Complexity Index; Casali et al., 2013).

In this case, the available equipment includes neuronavigated TMS (NBS4, Nexstim Plc, Finland) and a 64-channel DC EEG amplifier (BrainAmp, Brain Products GmbH, Germany). In particular, a 62-channel EEG cap with a 10–20 montage and two EOG channels placed with a diagonal montage are connected to the amplifier. Common physical reference and ground electrodes are placed on the forehead, i. e., far from the coil to avoid possible injection of TMS-related artifacts into the reference. Data are recorded at a 5 kHz sampling rate with DC-to-1000-Hz hardware filtering bandwidth and with 0.5 μV amplitude resolution. Skin preparation is performed to obtain < 5 kΩ impedance at all electrodes. rt-TEP is initialized with the IP address of the server computer (directly connected to the EEG amplifier), with the ordered set of channels streamed out by the amplifier, with the label of the TMS trigger, with the specification of the two EOG channels such that a bipolar signal is visualized, with the length of the time windows for RAW data check (i.e., 5 s) and for display of EEG responses to TMS both in single-trial and average mode (i.e., from –100 to 400 ms with respect to TMS onset time).

The operator starts by setting the stimulation site based on available anatomical information: using individual magnetic resonance images and a neuronavigated TMS system, she/he targets the premotor cortex a few centimeters left from the midline and orients the induced E-field orthogonally with respect to the underlying superior frontal gyrus. As a preliminary starting point, the operator also sets stimulation intensity at the resting motor threshold (rMT) previously assessed in the same subject, which is 38% of the maximum stimulator output (MSO) in this case. A masking noise is continuously played during TMS stimulation through in-ear earphones and titrated, within safety limits, in order to mask the coil's click. In this case, custom software (Russo et al., 2022) generating a device-specific and subject-specific masking noise is used; at the beginning of the experiment, few pulses are delivered while iteratively adjusting the noise parameters until the subject reports that the TMS click is not discernible.

The operator now delivers a few test pulses in the single-trial mode to identify and control artifacts potentially affecting the early post-stimulus time interval. The pulse artifact is checked in the rt-TEP single-trial mode and it is masked by setting the TMS-artifact time window from −2 ms to + 5 ms. Recharge artifact is prevented by setting the time of recharging of the stimulator's capacitors at 900 ms after the pulse. Discharge or muscle artifacts are minimized as described in the previous section (see Section 2.1) to obtain a clean view on the early components of single-trial TEP.

After switching to average mode, the operator starts a short block of 20 stimuli at a jittered inter-pulse interval of 2–2.3 s and observes, in
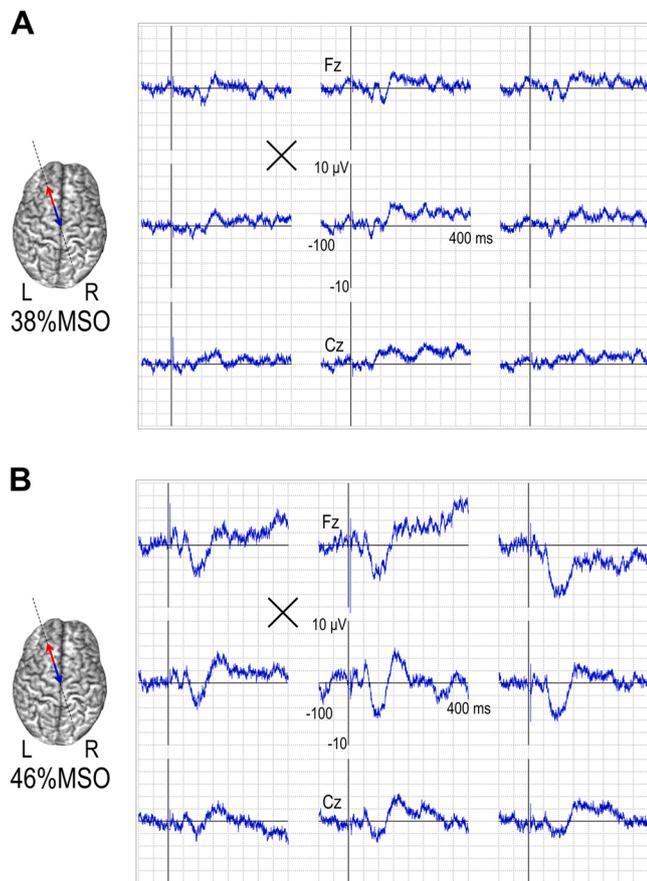
Fig. 4. 20-trial average EEG responses to TMS (zoom on frontocentral channels) when stimulating the same target on the left premotor cortex at 38% MSO (A) and 46% MSO (B). Stimulation parameters are also depicted on a rendered brain (left). EEG channels are displayed in the average reference. MSO = maximum stimulator output; L = left; R = right.

real time, the build-up of the EEG response on the rt-TEP monitor. Within a minute, the operator can appreciate the resulting average TEP (Fig. 4A) and notices that early (8–50 ms) components are absent or very small (V_{pp} below 2 µV) in the channels closest to the stimulation target (black cross), indicating that the parameters based on a priori information are not effective in eliciting an immediate local EEG response.

Thus, she/he decides to increase stimulation intensity to 46% MSO (corresponding to 120% rMT) and delivers another set of 20 pulses, while keeping the same coil position and orientation. Now, the operator detects the emergence of two new elements on the rt-TEP display (Fig. 4 B). First, early components in the channels closest to the stimulated site are detectable, although they are still smaller (V_{pp} about 4 µV in F1) with respect to the desired endpoint (10 µV) and lack a clear asymmetry between the two hemispheres. Second, she/he notices the appearance of negative–positive deflections between 100 and 200 ms. Their larger amplitude (V_{pp} about 6–8 µV) with respect to the early components and their central distribution, without any visible asymmetry related to the stimulation side, suggest the presence of auditory-evoked potentials (Nikouline et al., 1999).

Based on these two observations, the user decides to further increase stimulation intensity and to adjust noise masking, which was previously titrated to a lower intensity (i.e., 38% MSO). She/he thus sets the TMS intensity to 50% of the MSO and optimizes noise masking by increasing its level (always within safety limits) and/or by changing its spectral characteristics based on the subject's report (see Russo et al., 2022). After a new sequence of 20 pulses and another minute, the operator can appreciate the effects of the above-mentioned adjustments (Fig. 5A); early components in the channel closest to the stimulation site are larger
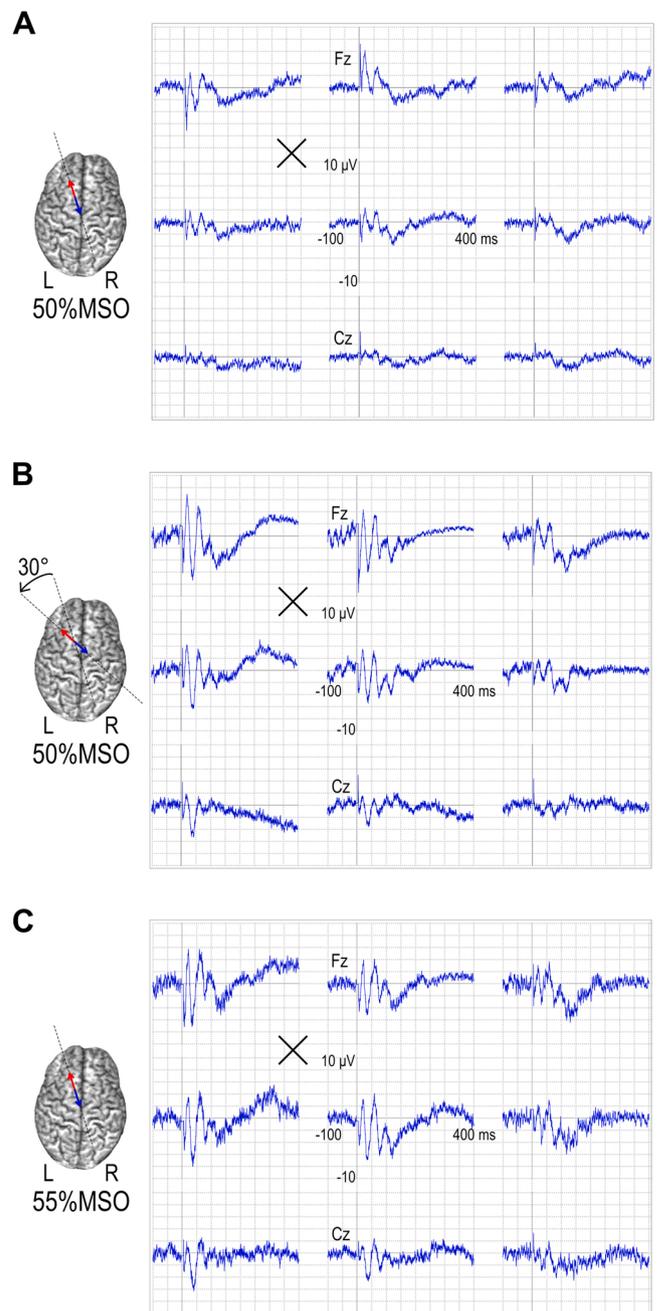
Fig. 5. 20-trial average EEG responses to TMS (zoom on frontocentral channels) when stimulating the same target on the left premotor cortex (black cross) at 50% MSO with a certain orientation (A), at 50% MSO after rotating the coil orientation by 30° counterclockwise (B) and at 55% MSO with the same coil orientation used in (A). Stimulation parameters are also depicted on a rendered brain (left). EEG channels are displayed in average reference. MSO = maximum stimulator output; L = left; R = right.

(V_{pp} about 7 µV in F1) and are followed by the emergence of fast oscillations, whereas the auditory-like N100–P200 sequence is obliterated. Overall, the response shows an asymmetric distribution, consistent with the stimulation of a left lateral target. Such real-time feedback suggests that the desired endpoint of $V_{pp} = 10$ µV is close and therefore only small adjustments are needed at this point.

To do this, the operator has different options: either increasing TMS intensity or changing the coil orientation, a modification that is known to have a significant impact on the immediate effects of TMS on the underlying circuits (Bonato et al., 2006; Casarotto et al., 2010; Tervo
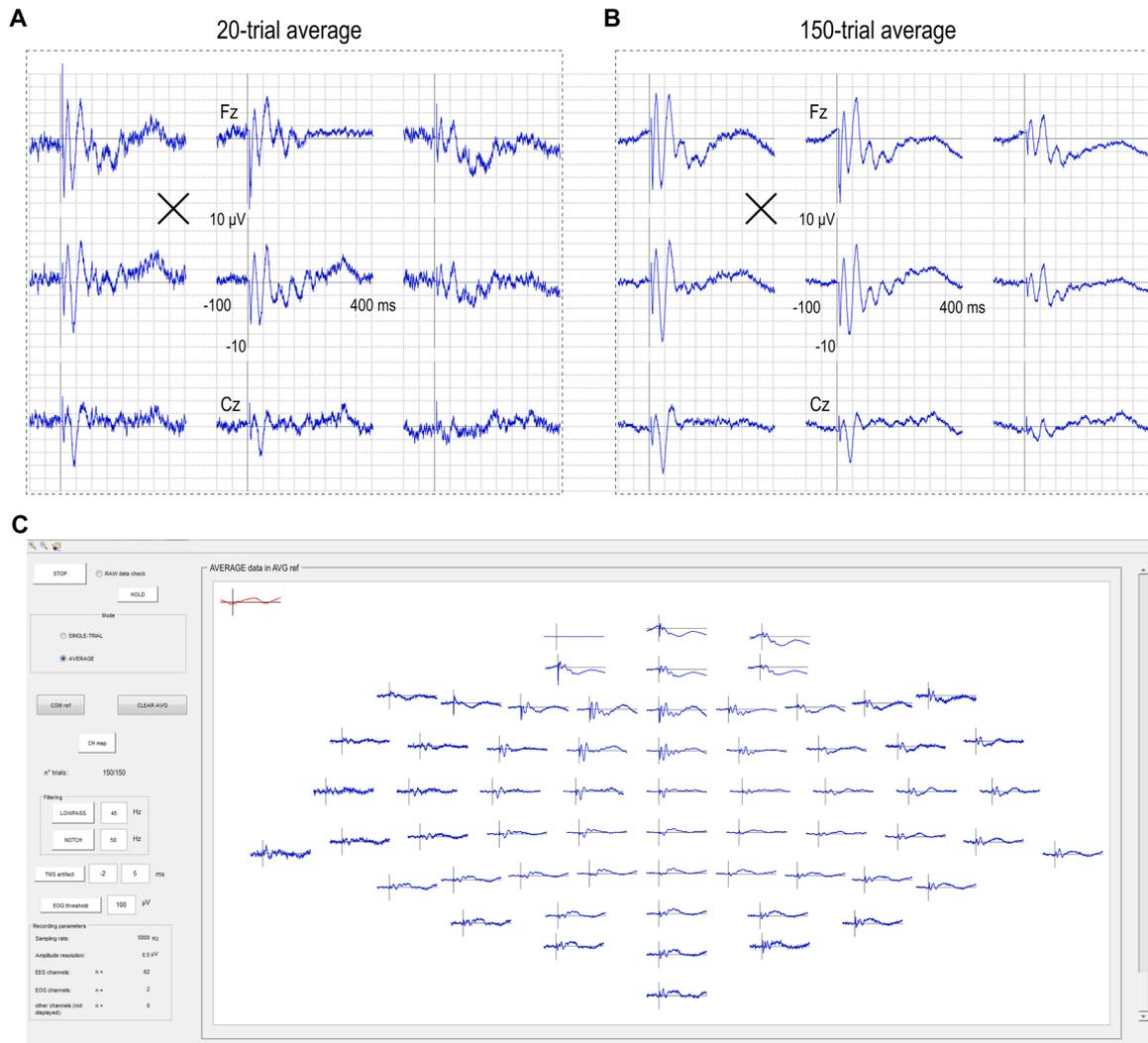
Fig. 6. EEG responses to TMS when stimulating the left premotor cortex (black cross) at 50% MSO with a certain orientation (as in Fig. 5B) after averaging 20 trials (A for a zoom on frontocentral channels) and 150 trials (B for a zoom on frontocentral channels, C for the all-channels display). EEG channels (blue trace) are displayed in average reference whereas EOG (red trace) is displayed in bipolar montage. MSO = maximum stimulator output.

et al., 2021). The operator considers exploring a different orientation as a first choice as this is less likely to require further adjustments of noise masking. She/he thus rotates the coil by 30° counterclockwise, while keeping the same intensity of 50% MSO. Delivering a new block of pulses confirms the effectiveness of this new parameter setting in achieving the desired endpoint (early components $V_{pp} > 10$ µV) as the rt-TEP monitor shows a high-amplitude early response at the site of stimulation (V_{pp} 14 µV in F1) (Fig. 5B). The operator now sets the stimulator to deliver a sequence of 150 pulses to perform data acquisition for subsequent analysis. Fig. 5C shows that similar results could have also been obtained, without rotating the coil, by increasing stimulation intensity by another 5% (i.e., 55% MSO).

Fig. 6 compares the TEPs obtained after averaging 20 trials to those obtained at the end of the session after averaging 150 trials (same parameters as in Fig. 5B). Here, one can note two important aspects. First, the amplitudes of the early and local components observed during the parameter search (average of 20 trials – Fig. 6A) is very close to their final value (average of 150 trials – Fig. 6B). Second, the parameter search results in TEPs whose waveform and features can be clearly appreciated in real time at the end of the experiment even before any further pre-processing step (e.g., off-line rejections, detrending, filtering, independent component analysis, etc.).

The importance of setting stimulation parameters before starting the

actual measurement, in order to optimize the initial cortical activation and to minimize obvious artifacts, is further illustrated in Fig. 7. This figure directly compares the final average TEPs (150 trials) collected during three sessions (corresponding, from top to bottom, to the stimulation parameters set in Figs. 4A, B and 5B). Although all these responses have been obtained by setting stimulation parameters based on reasonable a priori anatomical (position and orientation with respect to the cortical gyrus) and physiological (%MSO at or above rMT) assumptions, they differ in fundamental ways. The responses in Fig. 7A and B show absent/small early activations and are characterized by larger, late symmetric components which are maximal over midline channels, similar to those reported, for example, by (Conde et al., 2019; Chung et al., 2018). These waveforms are hardly consistent with the effects of direct cortical stimulation, which is expected to trigger responses that are large immediately after the pulse and specific for the stimulation site (Keller et al., 2014; Kundu et al., 2020). Conversely, the TEP reported in Fig. 7C fulfils these basic criteria and is similar to those described in previous studies (Casarotto et al., 2016; Rosanova et al., 2009; Sarasso et al., 2020; Sinitsyn et al., 2020). In this case, a strong initial activation is followed by an overall asymmetric wave shape with high SNR. As described above, reproducing this kind of responses only required maximizing the immediate impact of TMS on early (8–50 ms) components through slight adjustments of the intensity (5–10% MSO)
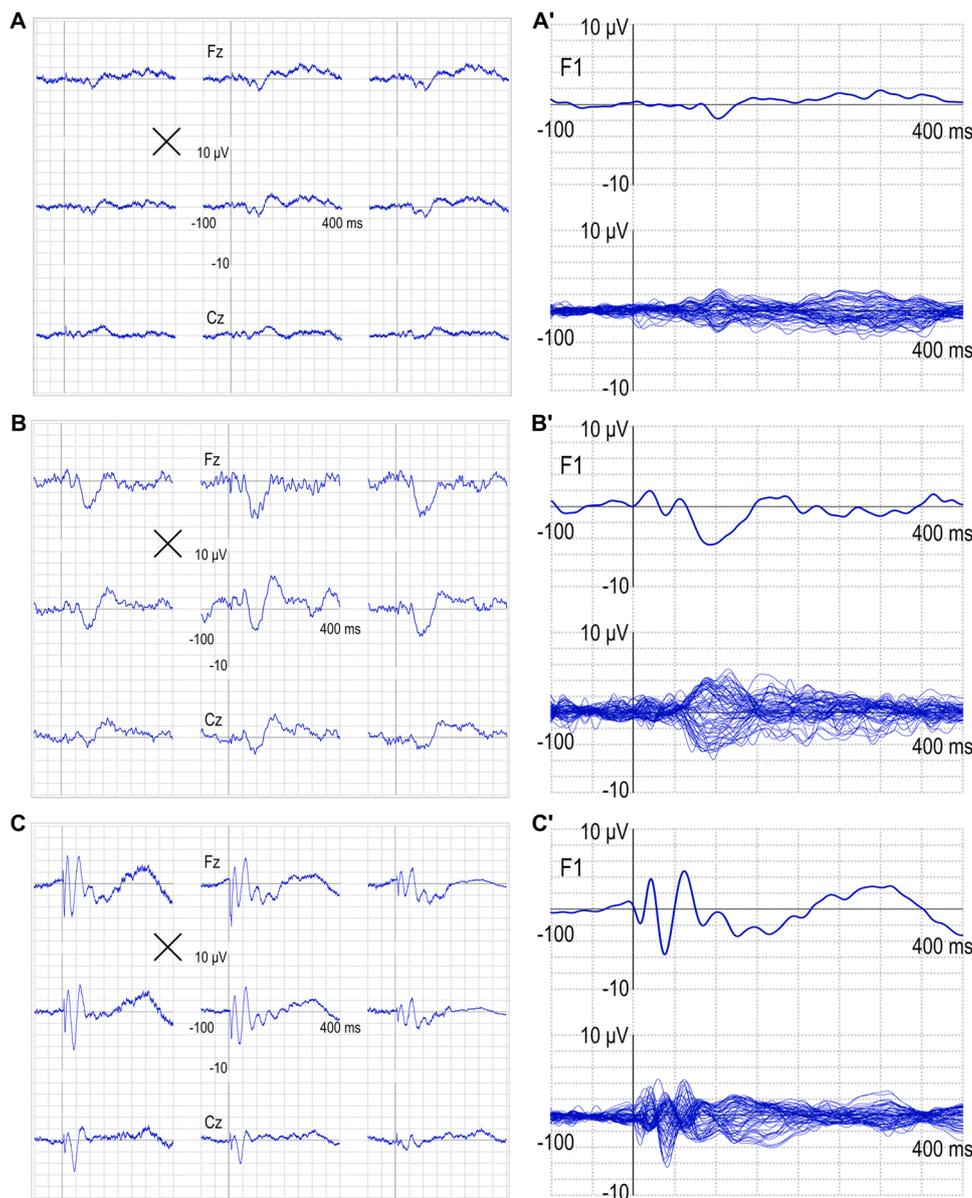
Fig. 7. 150-trial average EEG responses to TMS (zoom on frontocentral channels) when stimulating the same target on the left premotor cortex (black cross) at 38% MSO (A), at 46% MSO (B) and at 50% MSO with adjusted noise masking after rotating the coil orientation by 30° counterclockwise (C). See Figs. 4A, B and 5B for the corresponding 20-trial averages. EEG channels are displayed in the average reference. The corresponding F1 channel and butterfly plot (panels A', B' and C') have been low-pass filtered at 45 Hz. MSO = maximum stimulator output.

and/or the orientation of stimulation, while at the same time optimizing noise masking. Making such adjustments is relatively straightforward but would be impossible based on a priori information alone and can only be done if the operator is guided in real-time by an informative visual feedback about the immediate effects of TMS, such as the one provided by rt-TEP.

3. Discussion

With this paper, we introduce and release a novel tool to facilitate the acquisition of TEPs based on a real-time readout of the immediate impact of TMS on the underlying neuronal circuits. In short, rt-TEP guides the user through two sequential steps. The first step (i.e., single-trial mode) is used to detect and minimize artifacts potentially contaminating the early post-stimulus period. The second step (average mode) allows to adjust stimulation parameters until reaching the desired level of cortical activation, as judged by the peak-to-peak amplitude of early (8–50 ms) components elicited under the coil. In the experiment described in the present paper, we aimed at obtaining V_{pp} larger than 10 µV within the first 50 ms after the TMS pulse nearby the stimulation target, a specific endpoint that has been used in previous studies

(Casarotto et al., 2016; Rosanova et al., 2018; Sarasso et al., 2020; Sinitsyn et al., 2020). While this high level of initial cortical activation is a necessary feature to obtain TEPs with high SNR whereby the complexity of the spatiotemporal dynamics can be reliably computed for clinical purposes (PCI, Casali et al., 2013), it is important to stress that other experiments may require different (either smaller or larger initial components) endpoints, depending on the researchers' needs. For example, as we show in the Supplementary results section, the user may also choose to set the target amplitude based on more sophisticated data-driven criteria, such as by taking into account the variance of background EEG at the individual level. In this respect, the present paper is not meant to suggest a standard endpoint, but rather a general method to control and adjust the level of the initial input to the cerebral cortex using rt-TEP, as discussed below.

3.1. rt-TEP: rationale and applications

As we have recalled in the Introduction, the actual impact of the TMS-induced E-field on cortical neurons is very hard to predict based on a priori information. This problem is particularly relevant when targeting cortical sites outside the primary motor area for which the

immediate readout represented by the motor evoked potential (MEP) is not available. This lack of control on stimulation effectiveness may explain a significant portion of the large variability of TEP waveforms reported in the current literature. For example, while in many TMS–EEG studies TEPs are small in amplitude as well as symmetric and not specific for the cortical target, in others the stimulation of the same areas gives rise to very different responses that are larger in amplitude (up to one order of magnitude) as well as asymmetric and specific for the stimulated cortical site. As exemplified in Fig. 7, profoundly different responses can all be obtained within the envelope of reasonable parameter settings based on a priori information, such as individual anatomy and individual rMT. In fact, this variability (including instances in which no responses to TMS are detectable) likely reflects key factors that remain unaccounted for, including microscale axon orientation, cytoarchitectonic and local input–output properties of neurons.

The idea behind rt-TEP is that, while these factors remain hard to predict, it is possible to bypass this black box by controlling and adjusting stimulation parameters based on a post-hoc informed readout, i.e., the amplitude of early EEG components. In this perspective, rt-TEP extends to other cortical areas the same logic that normally applies to the primary motor cortex, in which adjustments of stimulation intensity are normally guided by the real-time assessment of MEPs. There are, however, specific challenges characterizing this EEG-based approach as compared to the classic MEP-based approach. First, early TMS-evoked EEG responses are harder to visualize than peripheral TMS-evoked EMG responses because they can be contaminated by various types of artifacts. Second, the actual readout is represented by a distribution of average potentials rather than by single-pulse EMG waves; this requires a dedicated visualization mode (i.e., average reference, topographic arrangement) to appreciate the spatial properties and the amplitude of the brain response. The key function of rt-TEP is to assist the operator in overcoming these problems through a customized visualization of the initial impact of TMS nearby the stimulated site. Once the initial cortical input is effective and complies with preset requirements (in the specific example reported here $V_{pp} > 10 \ \mu V$ within 8–50 ms after the pulse near the TMS target), the experimenter can analyze the overall brain's reaction to this focal perturbation for ultimately computing different quantitative indices. In this perspective, the initial level of cortical activation set with rt-TEP is the controlled experimental manipulation (the independent variable) whereas the ensuing evolution of the TEP, including its waveform, spectral content and specific spatiotemporal distribution is the observation (the dependent variable).

For example, once TMS parameters are set to effectively activate the underlying target, it is possible to appreciate the specificity of TEPs across different stimulation sites (Casarotto et al., 2010), to analyze the frequency content of the overall EEG response to the initial perturbation (i.e., the natural frequency; Rosanova et al., 2009), and how it may be altered in pathological conditions (Ferrarelli et al., 2008, 2012; Canali et al., 2015). As already mentioned, high signal-to-noise TEPs generated by effective perturbations can also be analyzed to derive brain complexity measures that are clinically useful to stratify patients with disorders of consciousness (Casali et al., 2013; Casarotto et al., 2016; Bodart et al., 2017; Sinitsyn et al., 2020). Likewise, ensuring effective stimulation is a key prerequisite to compare the electrophysiological properties of the stroke perilesional area to the ones of the contralateral site (Sarasso et al., 2020; Tscherpel et al., 2020). Finally, making sure that TMS is actually producing an initial effect on the underlying circuits, it is also an important prerequisite for experiments aimed at studying changes in cortical excitability in longitudinal or repeated measurements. In this case, the desired amplitude is set as the independent variable by means of rt-TEP only in the first experiment and then the exact stimulation parameters are repeated in the second measurements (ideally with the aid of a precise neuronavigation system) to see how the overall TEP, early components included (i.e., the dependent variable), changes after a given manipulation. Indeed, previous studies have shown that in control conditions (with no intervening

manipulation) once stimulation parameters are effective and kept fixed across repeated measurements, TEPs are highly reproducible in shape and amplitude (Casarotto et al., 2010; Lioumis et al., 2009) and they are also sensitive to spontaneous or induced changes in brain state. For example, TEPs can change upon falling asleep (Massimini et al., 2005, 2007), after sleep deprivation (Chellappa et al., 2016; Gaggioni et al., 2019, 2021; Huber et al., 2013; Ly et al., 2016), after the administration of anesthetics (Sarasso et al., 2015), electroconvulsive therapy (Casarotto et al., 2013), transcranial direct current stimulation (Romero Lauro et al., 2014), and neuroactive drugs such as L-Dopa (Casarotto et al., 2019; Turco et al., 2018).

3.2. rt-TEP: caveats and perspectives

A major limitation of TMS-EEG-based approaches in general is represented by unavoidable artifacts that can be present when stimulating cortical areas located directly below cranio-facial muscle insertions (Mutanen et al., 2013). The parameter search in rt-TEP single-trial mode is reliably successful in avoiding such artifacts when placing the coil over a large portion of the head; in our experience, a clean shot on early components can be easily obtained in correspondence of an area of the cortex spanning from Brodmann's area (BA) 18/19 to BA 6/9 and extending a few centimeters around the midline, including the hand motor areas (Rosanova et al., 2009; Casali et al., 2010; Ferrarelli et al., 2012; Fecchio et al., 2017). When stimulating more lateral cortical aspects, the user must necessarily make a compromise between data quality and the need for stimulating a specific circuit. Also in this case, rt-TEP can be useful as it allows the experimenter, already during the experiment, to make informed choices to achieve the optimal trade-off. Unfortunately, the likelihood of a satisfying balance may decrease markedly as the coil is moved anteriorly to dorsolateral prefrontal cortex (DLPFC) or posteriorly to BA 17 and may become extremely low on language areas.

Finally, the ultimate success of the overall rt-TEP procedure depends on the available hardware. For example, active amplifiers tend to induce early discharge artifacts that are more prominent and difficult to eliminate, often masking early components. Also, the accuracy of the TMS-navigation unit at hand is a key factor; indeed, the settings (coil position coordinates and rotation) identified during the parameter search in rt-TEP must be precisely retrieved and held steady throughout a single measurement and even more so across repeated measurements. Finally, TMS hardware, coils and pulse waveshapes can differ largely in their focality, efficacy on cortical circuits and collateral effects (magnetic artifacts, sensory and auditory stimulation) (Koponen et al., 2020; Van Doren et al., 2015). As major theoretical and technical efforts are currently ongoing to optimize these factors, rt-TEP may represent a useful tool to empirically explore and compare the pros and cons of the different solutions.

As described in this paper, in order to achieve effective stimulation, the adjustment of TMS parameters may involve, in addition to intensity changes, small coil rotations. Although a few manual rotations are generally effective in increasing early TEPs, a systematic search of the optimal E-field orientation is practically unfeasible. Such fine tuning requires more sophisticated strategies and hardware, such as for example an EEG-based adaptive search algorithm coupled with an electronically-controlled two-coil transducer (Souza et al., 2022; Tervo et al., 2020, 2021). Combining rt-TEP with advanced closed-loop systems represents a promising strategy whereby fundamental stimulation parameters are first set by the operator based on visual feedback and then automatically optimized in a closed-loop fashion.

3.3. rt-TEP: why to use it

The tool presented in this paper offers an informative sequence of simple visualization modes to facilitate the successful acquisition of TEPs that is not currently implemented in any commercial software.

Below, we would like to highlight key reasons that should motivate the incorporation of rt-TEP in future experimental designs.

First and foremost, researchers and clinicians alike would like to avoid situations such as that illustrated in Fig. 7A where, in spite of reasonable a priori assumptions, TMS has no or little impact on the underlying cortex. Such occurrences, which represent a clear drawback not only for TMS–EEG studies but also for interventional protocols (plasticity), can be readily controlled for and prevented with rt-TEP.

Second, aligning the initial effects of TMS (the independent variable) within a given range across studies and laboratories may mitigate the problem of reproducibility currently affecting the TMS–EEG literature (Belardinelli et al., 2019).

Third, rt-TEP allows increasing the cortical impact of TMS in ways (small coil translation and rotations) that do not necessarily involve, or that minimize, the need for large increases of stimulation intensity (Fig. 5B). Such optimization of the effects of genuine cortical activation over the collateral sensory effects of the coil's discharge is key to improve the quality and informativeness of TEPs.

Fourth, through a series of visualization steps, rt-TEP guides the operator in eliminating/minimizing obvious artifacts and confounding factors during data collection, including muscle twitches and auditory evoked potentials, which must be otherwise eliminated during post processing. This is an important advantage, in view of the possible sensory input associated with muscle twitches and considering the limitations inherent to many off-line artifact rejection algorithms (such as principal component analysis - PCA and independent component analysis - ICA) (Biabani et al., 2019; Belardinelli et al., 2019; Bertazzoli et al., 2021).

Finally, rt-TEP provides the experimenter with clear, real-time feedback about data quality already during the experiment (Fig. 6). This prevents discovering poor TEP quality only at a later stage and after time-consuming post-processing, which is particularly problematic when a second measurement is not an option, as it is often the case in patients.

More generally, real-time feedback about the effect of TMS on the underlying tissue may render TMS–EEG more reliable and akin to other measuring tools that have proven to be extremely powerful in medicine. As exemplified in this paper, the TMS probe, just like an ultrasound probe, requires informed handling in order to recover a strong signal of interest amidst layers of noise. In daily practice, echography operators are involved in a similar task; they orient the probe until they recover on their monitors a robust echo from the target structure; when basic SNR criteria are met, only then can the actual measurement start. Thanks to an effective real-time readout and with some practice, these operator-dependent procedures become second nature and reliable to the point of supporting important medical decisions. By comparison, TMS–EEG is still in its infancy, but we hope that the release of rt-TEP software may represent a step further in this direction.

Declarations of interest

none.

Acknowledgment

Appendix A. Supporting information

Supplementary data associated with this article can be found in the online version at doi:10.1016/j.jneumeth.2022.109486.

References

Belardinelli, P., Biabani, M., Blumberger, D.M., Bortoletto, M., Casarotto, S., David, O., Desideri, D., Etkin, A., Ferrarelli, F., Fitzgerald, P.B., Fornito, A., Gordon, P.C., Gosseries, O., Harquel, S., Julkunen, P., Keller, C.J., Kimiskidis, V.K., Lioumis, P., Miniussi, C., Rosanova, M., Rossi, S., Sarasso, S., Wu, W., Zrenner, C., Daskalakis, Z. J., Rogasch, N.C., Massimini, M., Ziemann, U., Ilmoniemi, R.J., 2019. Reproducibility in TMS–EEG studies: A call for data sharing, standard procedures and effective experimental control. Brain Stimul. 12, 787–790. https://doi.org/10.1016/j.brs.2019.01.010.

Bertazzoli, G., Esposito, R., Mutanen, T.P., Ferrari, C., Ilmoniemi, R.J., Miniussi, C., Bortoletto, M., 2021. The impact of artifact removal approaches on TMS–EEG signal. Neuroimage 239, 118272. https://doi.org/10.1016/j.neuroimage.2021.118272.

Biabani, M., Fornito, A., Mutanen, T.P., Morrow, J., Rogasch, N.C., 2019. Characterizing and minimizing the contribution of sensory inputs to TMS-evoked potentials. Brain Stimul. 12, 1537–1552. https://doi.org/10.1016/j.brs.2019.07.009.

Bodart, O., Gosseries, O., Wannez, S., Thibaut, A., Annen, J., Boly, M., Rosanova, M., Casali, A.G., Casarotto, S., Tononi, G., Massimini, M., Laureys, S., 2017. Measures of metabolism and complexity in the brain of patients with disorders of consciousness. Neuroimage Clin. 14, 354–362. https://doi.org/10.1016/j.nicl.2017.02.002.

Bonato, C., Miniussi, C., Rossini, P.M., 2006. Transcranial magnetic stimulation and cortical evoked potentials: A TMS/EEG co-registration study. Clin. Neurophysiol. 117, 1699–1707. https://doi.org/10.1016/j.clinph.2006.05.006.

Canali, P., Sarasso, S., Rosanova, M., Casarotto, S., Sferrazza-Papa, G., Gosseries, O., Fecchio, M., Massimini, M., Mariotti, M., Cavallaro, R., Smeraldi, E., Colombo, C., Benedetti, F., 2015. Shared reduction of oscillatory natural frequencies in bipolar disorder, major depressive disorder and schizophrenia. J. Affect. Disord. 184, 111–115. https://doi.org/10.1016/j.jad.2015.05.043.

Casali, A.G., Casarotto, S., Rosanova, M., Mariotti, M., Massimini, M., 2010. General indices to characterize the electrical response of the cerebral cortex to TMS. Neuroimage 49, 1459–1468. https://doi.org/10.1016/j.neuroimage.2009.09.026.

Casali, A.G., Gosseries, O., Rosanova, M., Boly, M., Sarasso, S., Casali, K.R., Casarotto, S., Bruno, M.-A., Laureys, S., Tononi, G., Massimini, M., 2013. A theoretically based index of consciousness independent of sensory processing and behavior. Sci. Transl. Med. 5 https://doi.org/10.1126/scitranslmed.3006294.

Casarotto, S., Canali, P., Rosanova, M., Pigorini, A., Fecchio, M., Mariotti, M., Lucca, A., Colombo, C., Benedetti, F., Massimini, M., 2013. Assessing the effects of electroconvulsive therapy on cortical excitability by means of transcranial magnetic stimulation and electroencephalography. Brain Topogr. 26, 326–337. https://doi.org/10.1007/s10548-012-0256-8.

Casarotto, S., Comanducci, A., Rosanova, M., Sarasso, S., Fecchio, M., Napolitani, M., Pigorini, A., Casali, A.G., Trimarchi, P.D., Boly, M., Gosseries, O., Bodart, O., Curto, F., Landi, C., Mariotti, M., Devalle, G., Laureys, S., Tononi, G., Massimini, M., 2016. Stratification of unresponsive patients by an independently validated index of brain complexity. Ann. Neurol. 80, 718–729. https://doi.org/10.1002/ana.24779.

Casarotto, S., Romero Lauro, L.J., Bellina, V., Casali, A.G., Rosanova, M., Pigorini, A., Defendi, S., Mariotti, M., Massimini, M., 2010. EEG responses to TMS are sensitive to changes in the perturbation parameters and repeatable over time. PLoS ONE 5, e10281. https://doi.org/10.1371/journal.pone.0010281.

Casarotto, S., Turco, F., Comanducci, A., Perretti, A., Marotta, G., Pezzoli, G., Rosanova, M., Isaias, I.U., 2019. Excitability of the supplementary motor area in Parkinson's disease depends on subcortical damage. Brain Stimul. 12, 152–160. https://doi.org/10.1016/j.brs.2018.10.011.

Chellappa, S.L., Gaggioni, G., Ly, J.Q.M., Papachilleos, S., Borsu, C., Brzozowski, A., Rosanova, M., Sarasso, S., Luxen, A., Middleton, B., Archer, S.N., Dijk, D.-J., Massimini, M., Maquet, P., Phillips, C., Moran, R.J., Vandewalle, G., 2016. Circadian dynamics in measures of cortical excitation and inhibition balance. Sci. Rep. 6, 33661. https://doi.org/10.1038/srep33661.

Chung, S.W., Rogasch, N.C., Hoy, K.E., Fitzgerald, P.B., 2018. The effect of single and repeated prefrontal intermittent theta burst stimulation on cortical reactivity and working memory. Brain Stimul. 11, 566–574. https://doi.org/10.1016/j.brs.2018.01.002.

Conde, V., Tomasevic, L., Akopian, I., Stanek, K., Saturnino, G.B., Thielscher, A., Bergmann, T.O., Siebner, H.R., 2019. The non-transcranial TMS-evoked potential is an inherent source of ambiguity in TMS-EEG studies. Neuroimage 185, 300–312. https://doi.org/10.1016/j.neuroimage.2018.10.052.

Fecchio, M., Pigorini, A., Comanducci, A., Sarasso, S., Casarotto, S., Premoli, I., Derchi, C.-C., Mazza, A., Russo, S., Resta, F., Ferrarelli, F., Mariotti, M., Ziemann, U., Massimini, M., Rosanova, M., 2017. The spectral features of EEG responses to transcranial magnetic stimulation of the primary motor cortex depend on the amplitude of the motor evoked potentials. PLoS ONE 12, e0184910. https://doi.org/10.1371/journal.pone.0184910.

Ferrarelli, F., Massimini, M., Peterson, M.J., Riedner, B.A., Lazar, M., Murphy, M.J., Huber, R., Rosanova, M., Alexander, A.L., Kalin, N., Tononi, G., 2008. Reduced evoked gamma oscillations in the frontal cortex in schizophrenia patients: a TMS/EEG study. Am. J. Psychiatry 165, 996–1005. https://doi.org/10.1176/appi.ajp.2008.07111733.

Ferrarelli, F., Sarasso, S., Guller, Y., Riedner, B.A., Peterson, M.J., Bellesi, M., Massimini, M., Postle, B.R., Tononi, G., 2012. Reduced natural oscillatory frequency

of frontal thalamocortical circuits in schizophrenia. Arch. Gen. Psychiatry 69, 766–774. https://doi.org/10.1001/archgenpsychiatry.2012.147.

Freche, D., Naim-Feil, J., Peled, A., Levit-Binnun, N., Moses, E., 2018. A quantitative physical model of the TMS-induced discharge artifacts in EEG. PLOS Comput. Biol. 14, e1006177 https://doi.org/10.1371/journal.pcbi.1006177.

Gaggioni, G., Ly, J.Q.M., Muto, V., Chellappa, S.L., Jaspar, M., Meyer, C., Delfosse, T., Vanvinckenroye, A., Dumont, R., Coppieters 't Wallant, D., Berthomier, C., Narbutas, J., Van Egroo, M., Luxen, A., Salmon, E., Collette, F., Phillips, C., Schmidt, C., Vandewalle, G., 2019. Age-related decrease in cortical excitability circadian variations during sleep loss and its links with cognition. Neurobiol. Aging 78, 52–63. https://doi.org/10.1016/j.neurobiolaging.2019.02.004.

Gaggioni, G., Shumbayawonda, E., Montanaro, U., Ly, J.Q.M., Phillips, C., Vandewalle, G., Abásolo, D., 2021. Time course of cortical response complexity during extended wakefulness and its differential association with vigilance in young and older individuals. Biochem. Pharmacol. 191, 114518 https://doi.org/10.1016/j.bcp.2021.114518.

Huber, R., Mäki, H., Rosanova, M., Casarotto, S., Canali, P., Casali, A.G., Tononi, G., Massimini, M., 2013. Human cortical excitability increases with time awake. Cereb. Cortex 23, 332–338. https://doi.org/10.1093/cercor/bhs014.

Keller, C.J., Honey, C.J., Entz, L., Bickel, S., Groppe, D.M., Toth, E., Ulbert, I., Lado, F.A., Mehta, A.D., 2014. Corticocortical evoked potentials reveal projectors and integrators in human nrain networks. J. Neurosci. 34, 9152–9163. https://doi.org/10.1523/JNEUROSCI.4289-13.2014.

Koponen, L.M., Nieminen, J.O., Ilmoniemi, R.J., 2015. Minimum-energy coils for transcranial magnetic stimulation: application to focal stimulation. Brain Stimul. 8, 124–134. https://doi.org/10.1016/j.brs.2014.10.002.

Koponen, L.M., Goetz, S.M., Tucci, D.L., Peterchev, A.V., 2020. Sound comparison of seven TMS coils at matched stimulation strength. Brain Stimul. 13, 873–880. https://doi.org/10.1016/j.brs.2020.03.004.

Kundu, B., Davis, T.S., Philip, B., Smith, E.H., Arain, A., Peters, A., Newman, B., Butson, C.R., Rolston, J.D., 2020. A systematic exploration of parameters affecting evoked intracranial potentials in patients with epilepsy. Brain Stimul. 13, 1232–1244. https://doi.org/10.1016/j.brs.2020.06.002.

Lei, X., Liao, K., 2017. Understanding the influences of EEG reference: a large-scale brain network perspective. Front. Neurosci. 11, 205. https://doi.org/10.3389/fnins.2017.00205.

Lioumis, P., Kičić, D., Savolainen, P., Mäkelä, J.P., Kähkönen, S., 2009. Reproducibility of TMS-evoked EEG responses. Hum. Brain Mapp. 30 (4), 1387–1396. https://doi.org/10.1002/hbm.20608.

Ly, J.Q.M., Gaggioni, G., Chellappa, S.L., Papachilleos, S., Brzozowski, A., Borsu, C., Rosanova, M., Sarasso, S., Middleton, B., Luxen, A., Archer, S.N., Phillips, C., Dijk, D.-J., Maquet, P., Massimini, M., Vandewalle, G., 2016. Circadian regulation of human cortical excitability. Nat. Commun. 7, 11828. https://doi.org/10.1038/ncomms11828.

Mäki, H., Ilmoniemi, R.J., 2011. Projecting out muscle artifacts from TMS-evoked EEG. Neuroimage 54, 2706–2710. https://doi.org/10.1016/j.neuroimage.2010.11.041.

Massimini, M., Ferrarelli, F., Esser, S.K., Riedner, B.A., Huber, R., Murphy, M., Peterson, M.J., Tononi, G., 2007. Triggering sleep slow waves by transcranial magnetic stimulation. Proc. Natl. Acad. Sci. U.S.A. 104, 8496–8501. https://doi.org/10.1073/pnas.0702495104.

Massimini, M., Ferrarelli, F., Huber, R., Esser, S.K., Singh, H., Tononi, G., 2005. Breakdown of cortical effective connectivity during sleep. Science 309, 2228–2232. https://doi.org/10.1126/science.1117256.

Mutanen, T., Mäki, H., Ilmoniemi, R.J., 2013. The effect of stimulus parameters on TMS–EEG muscle artifacts. Brain Stimul. 6, 371–376. https://doi.org/10.1016/j.brs.2012.07.005.

Nikouline, V., Ruohonen, J., Ilmoniemi, R.J., 1999. The role of the coil click in TMS assessed with simultaneous EEG. Clin. Neurophysiol. 110, 1325–1328. https://doi.org/10.1016/S1388-2457(99)00070-X.

Nunez, P.L., 2010. REST: A good idea but not the gold standard. Clin. Neurophysiol. 121, 2177–2180. https://doi.org/10.1016/j.clinph.2010.04.029.

Nunez, P.L., Srinivasan, R., 2006. A theoretical basis for standing and traveling brain waves measured with human EEG with implications for an integrated consciousness. Clin. Neurophysiol. 117, 2424–2435. https://doi.org/10.1016/j.clinph.2006.06.754.

Rocchi, L., Di Santo, A., Brown, K., Ibáñez, J., Casula, E., Rawji, V., Di Lazzaro, V., Koch, G., Rothwell, J., 2021. Disentangling EEG responses to TMS due to cortical and peripheral activations. Brain Stimul. 14, 4–18. https://doi.org/10.1016/j.brs.2020.10.011.

Romero Lauro, L.J., Rosanova, M., Mattavelli, G., Convento, S., Pisoni, A., Opitz, A., Bolognini, N., Vallar, G., 2014. TDCS increases cortical excitability: Direct evidence from TMS–EEG. Cortex 58, 99–111. https://doi.org/10.1016/j.cortex.2014.05.003.

Rosanova, M., Casali, A.G., Bellina, V., Resta, F., Mariotti, M., Massimini, M., 2009. Natural frequencies of human corticothalamic circuits. J. Neurosci. 29, 7679–7685. https://doi.org/10.1523/JNEUROSCI.0445-09.2009.

Rosanova, M., Fecchio, M., Casarotto, S., Sarasso, S., Casali, A.G., Pigorini, A., Comanducci, A., Seregni, F., Devalle, G., Citerio, G., Bodart, O., Boly, M., Gosseries, O., Laureys, S., Massimini, M., 2018. Sleep-like cortical OFF-periods disrupt causality and complexity in the brain of unresponsive wakefulness syndrome patients. Nat. Commun. 9, 4427. https://doi.org/10.1038/s41467-018-06871-1.

Rossini, P.M., Burke, D., Chen, R., Cohen, L.G., Daskalakis, Z., Di Iorio, R., Di Lazzaro, V., Ferreri, F., Fitzgerald, P.B., George, M.S., Hallett, M., Lefaucheur, J.P., Langguth, B., Matsumoto, H., Miniussi, C., Nitsche, M.A., Pascual-Leone, A., Paulus, W., Rossi, S., Rothwell, J.C., Siebner, H.R., Ugawa, Y., Walsh, V., Ziemann, U., 2015. Non-invasive electrical and magnetic stimulation of the brain, spinal cord, roots and peripheral nerves: Basic principles and procedures for routine clinical and research application. An updated report from an I.F.C.N. Committee. Clin. Neurophysiol. 126, 1071–1107. https://doi.org/10.1016/j.clinph.2015.02.001.

Russo, S., Sarasso, S., Puglisi, G.E., Dal Palù, D., Pigorini, A., Casarotto, S., D'Ambrosio, S., Astolfi, A., Massimini, M., Rosanova, M., Fecchio, M., 2022. TAAC - TMS Adaptable Auditory Control: A universal tool to mask TMS clicks. J. Neurosci. Methods, 109491. https://doi.org/10.1016/j.jneumeth.2022.109491. In this issue.

Sarasso, S., Boly, M., Napolitani, M., Gosseries, O., Charland-Verville, V., Casarotto, S., Rosanova, M., Casali, A.G., Brichant, J.-F., Boveroux, P., Rex, S., Tononi, G., Laureys, S., Massimini, M., 2015. Consciousness and complexity during unresponsiveness induced by propofol, xenon, and ketamine. Curr. Biol. 25, 3099–3105. https://doi.org/10.1016/j.cub.2015.10.014.

Sarasso, S., D'Ambrosio, S., Fecchio, M., Casarotto, S., Viganò, A., Landi, C., Mattavelli, G., Gosseries, O., Quarenghi, M., Laureys, S., Devalle, G., Rosanova, M., Massimini, M., 2020. Local sleep-like cortical reactivity in the awake brain after focal injury. Brain 143, 3672–3684. https://doi.org/10.1093/brain/awaa338.

Silva, L.M., Silva, K.M.S., Lira-Bandeira, W.G., Costa-Ribeiro, A.C., Araújo-Neto, S.A., 2021. Localizing the primary motor cortex of the hand by the 10-5 and 10-20 systems for neurostimulation: an MRI study. Clin. EEG Neurosci. 52 (6), 427–435. https://doi.org/10.1177/1550059420934590.

Sinitsyn, D.O., Poydasheva, A.G., Bakulin, I.S., Legostaeva, L.A., Iazeva, E.G., Sergeev, D. V., Sergeeva, A.N., Kremneva, E.I., Morozova, S.N., Lagoda, D.Yu, Casarotto, S., Comanducci, A., Ryabinkina, Y.V., Suponeva, N.A., Piradov, M.A., 2020. Detecting the potential for consciousness in unresponsive patients using the Perturbational Complexity Index. Brain Sci. 10, 917. https://doi.org/10.3390/brainsci10120917.

Souza, V.H., Nieminen, J.O., Tugin, S., Koponen, L., Baffa, O., Ilmoniemi, R.J., 2022. TMS with fast and accurate electronic control: measuring the orientation sensitivity of corticomotor pathways. Brain Stimul. https://doi.org/10.1016/j.brs.2022.01.009. In press.

Tervo, A.E., Metsomaa, J., Nieminen, J.O., Sarvas, J., Ilmoniemi, R.J., 2020. Automated search of stimulation targets with closed-loop transcranial magnetic stimulation. Neuroimage 220, 117082. https://doi.org/10.1016/j.neuroimage.2020.117082.

Tervo, A.E., Nieminen, J.O., Lioumis, P., Metsomaa, J., Souza, V.H., Sinisalo, H., Stenroos, M., Sarvas, J., Ilmoniemi, R.J., 2021. Closed-loop optimization of transcranial magnetic stimulation with electroencephalography feedback. bioRxiv. https://doi.org/10.1101/2021.08.31.458148.

Tscherpel, C., Dern, S., Hensel, L., Ziemann, U., Fink, G.R., Grefkes, C., 2020. Brain responsivity provides an individual readout for motor recovery after stroke. Brain 143, 1873–1888. https://doi.org/10.1093/brain/awaa127.

Turco, F., Canessa, A., Olivieri, C., Pozzi, N.G., Palmisano, C., Arnulfo, G., Marotta, G., Volkmann, J., Pezzoli, G., Isaias, I.U., 2018. Cortical response to levodopa in Parkinson's disease patients with dyskinesias. Eur. J. Neurosci. 48, 2362–2373. https://doi.org/10.1111/ejn.14114.

Van Doren, J., Langguth, B., Schecklmann, M., 2015. TMS-related potentials and artifacts in combined TMS-EEG measurements: Comparison of three different TMS devices. Neurophysiol. Clin. 45, 159–166. https://doi.org/10.1016/j.neucli.2015.02.002.

Virtanen, J., Ruohonen, J., Näätänen, R., Ilmoniemi, R.J., 1999. Instrumentation for the measurement of electric brain responses to transcranial magnetic stimulation. Med. Biol. Eng. Comput. 37, 322–326. https://doi.org/10.1007/BF02513307.

Yao, D., Qin, Y., Hu, S., Dong, L., Bringas Vega, M.L., Valdés Sosa, P.A., 2019. Which reference should we use for EEG and ERP practice? Brain Topogr. 32, 530–549. https://doi.org/10.1007/s10548-019-00707-x.